Transmission Lines on Alumina Ribbon Ceramic Substrate Material for 30 to 170 GHz Wireless Applications

Nahid Aslani-Amoli[1], Mutee Ur Rehman[1], Sridhar Sivapurapu[1], Fuhan Liu[1], Madhavan Swaminathan[1*], Cheng-Gang Zhuang[2], Nikolay Z. Zhelev[2], Seong-ho Seok[2], Cheolbok Kim[2]
[1]3D Systems Packaging Research Center (PRC), School of Electrical and Computer Engineering, Georgia Institute of Technology, Atlanta, GA, USA
[*]School of Materials Science and Engineering, Georgia Institute of Technology, Atlanta, GA, USA
[2]Corning Incorporated, Corning, NY, USA

Abstract— **New material technologies must be explored to realize high-performance packages for meeting the stringent requirements defined in the fifth generation (5G) and sub-THz frequency bands. To this end, electrical properties of the new materials such as dielectric constant (relative permittivity) and loss tangent need to be characterized along with the loss of interconnects on these substrates to investigate their suitability for mm-wave applications. In this paper, a newly developed material technology at Corning, namely, Alumina Ribbon Ceramic is introduced, and 40-µm-thick Alumina Ribbon Ceramic is characterized in the frequency range of 30-170 GHz using microstrip ring resonator (MRR) method. In addition, various planar transmission lines such as microstrip and coplanar waveguide (CPW) lines are designed and fabricated on a 40-µm-thick Alumina Ribbon Ceramic using a Semi-Additive Patterning (SAP) process to evaluate the performance of interconnects in decibels per millimeter (dB/mm) up to 170 GHz. Based on the measurements, the dielectric constant of Alumina Ribbon Ceramic is found to be steady around 9.87 and the extracted loss tangent varies from 0.0003 to 0.0013 in 30-170 GHz. Moreover, the average measured insertion loss of microstrip lines is between 0.089 dB/mm to 0.29 dB/mm from 30 GHz to 170 GHz. For the CPW lines, the average measured insertion loss varies from 0.053 dB/mm to 0.242 dB/mm in 30-170 GHz. According to the comparisons made with state-of-the-art substrate technologies, the CPW lines on Alumina Ribbon Ceramic exhibit the best performance in terms of loss (dB/mm) up to 170 GHz. These results demonstrate the excellent electrical properties of Alumina Ribbon Ceramic substrates for applications in 5G and sub-THz frequency bands.**

Keywords—Alumina Ribbon Ceramic, D-band, dielectric constant, loss tangent, microstrip ring resonator, millimeter-wave frequencies, transmission line losses

I. Introduction

Owing to increasing demands for higher data-rates, wider bandwidth, and lower latency to support new applications such as virtual reality (VR) and augmented reality (AR) emerged recently, 4G LTE wireless communication systems has faced unique challenges both in the component and package levels in terms of design complexities and stringent performance requirements. 5G wireless networks as a panacea for all these difficulties call for innovative design and substrate packaging technologies to be able to serve end-users through mm-wave frequency ranges. The heterogeneous integration required in packaging of 5G systems necessitates integration of active and passive components along with RF, analog, and digital functions in a single module which poses new challenges to the packaging designers from the standpoint of size, performance, and heat dissipation. Therefore, adoption of new packaging architectures demands for advanced materials to meet the new requirements imposed by 5G networks. For instance, for antenna-in-package (AiP), the low-loss dielectric material alleviates the dielectric loss in in-package interconnects, feedlines, and antennas, thus improving the antenna efficiency. Additionally, tackling thermal management issues regarding the high losses in the power amplifiers (PAs) when integrating with antenna arrays and miniaturization required for component integration can be addressed through developing new substrate material technologies [1,2]. The need to satisfy 5G requirements is intensified when the sixth generation (6G) wireless networks are around the corner, meeting the demands for a fully connected, intelligent digital world [3].

Knowing the accurate electrical properties of substrate materials such as dielectric constant and loss tangent is essential for designing efficient passive components such as transmission lines, filters, and antennas. For this reason, in the recent decade, tremendous research efforts have focused on characterizing dielectric materials to extract their electrical properties using various methods such as parallel plate method, free space method, cavity resonators, and transmission line techniques which consist of microstrip and coplanar waveguide (CPW) lines, ring resonators and T-resonators to name a few. Each of these methods has its own limitations and advantages corresponding to the frequency band on interest [4]. Among them, the microstrip ring resonator (MRR) method has been widely used in the literature for characterizing substrate materials like polymer/glass/polymer [5, 6], liquid crystal polymer (LCP) [7, 8], and low temperature co-fired ceramic (LTCC) [9] over a broad frequency ranges up to 110 GHz and in 110-170 GHz (D-band). Besides, the insertion loss of various

2377-5726/21/$31.00 ©2021 IEEE

DOI 10.1109/ECTC32696.2021.00356

planar transmission lines such as microstrip (MS), CPW, and conductor-backed coplanar waveguide (CBCPW) lines on state-of-the-art substrate technologies has been characterized in decibels per unit length up to 170 GHz to evaluate their performance for 5G and sub-THz packaging applications [5-7], [10, 11].

In parallel with the research efforts made in academia to identify and characterize new materials for 5G and beyond, some major attempts have also been made at the industry side to develop new materials. For instance, Corning has recently developed and introduced the Alumina Ribbon Ceramic material at Ceramic Expo. 2019 as an ultra-thin, flexible ceramic substrate available in wafer, panel, or long ribbon form. Important characteristics of this material include high dielectric constant, high dielectric strength, low loss tangent, and high thermal conductivity, which make it a good choice for future 5G packaging technologies. Moreover, its high flexural strength enables realizing packaging for sensors that conform to curved surfaces [12]. The measured dielectric constant and loss tangent of the Alumina Ribbon Ceramic based on an Fabry-Perot open cavity from 10 to 60 GHz have been reported as ~10 and ~0.0001, respectively [12]. Given the interesting characteristics of Alumina Ribbon Ceramic, not much is known about its electrical properties over a broad range of frequencies in the mm-wave and sub-mmwave frequency ranges. In this work, we report the first results of Alumina Ribbon Ceramic's characterization in the 30-170 GHz frequency band using MRR method. In addition, the insertion loss of MS and CPW transmission lines fabricated on Alumina Ribbon Ceramic using the semi-additive patterning (SAP) process is characterized up to 170 GHz. The material stack-up used for fabricating MRRs and transmission lines is a 40-µm-thick substrate.

Given its excellent material properties, Alumina Ribbon Ceramic substrates can be utilized to address the unique challenges introduced in 5G and beyond packaging technologies. Its higher dielectric constant and very low loss tangent combined with its high thermal conductivity provide an appealing opportunity for advancements in substrate packaging to realize ultra-miniaturized, high-performance passive components and tackle the thermal management issues posed in heterogeneous integration of passive and active components and modules in 5G mm-wave frequency region. The main purpose of this paper is to explore the suitability of Alumina Ribbon Ceramic material for 5G and sub-THz packaging application and demonstrate its competency through comparisons with state-of-the-art substrate technologies.

The remainder of this paper is structured as follows. Section II presents the design parameters of microstrip ring resonators (MRRs) and transmission lines on the 40-µm-thick Alumina Ribbon Ceramic. The fabrication process of the designed structures is explained in Section III, followed by analyzing measurement results in 30-170 GHz provided in Section IV. The performance of Alumina Ribbon Ceramic-based interconnects with state-of-the-art substrate technologies is compared and discussed in Section V. Finally, concluding remarks are given in Section VI.

II. Design of Structures

Microstrip ring resonators and planar transmission lines (microstrip and CPW) are designed on a 40-µm-thick Alumina Ribbon Ceramic substrate to characterize the electrical properties of Alumina Ribbon Ceramic in 30-170 GHz and evaluate the performance of Alumina Ribbon Ceramic-based interconnects up to 170 GHz as well. The electrical properties of Alumina Ribbon Ceramic reported in [12] are utilized in the design process of all test structures, carried out in ANSYS HFSS v19.3 [13].

A. Microstrip Ring Resonators

Resonator-based methods are among well-stablished approaches to characterize the low loss material technologies over a broad range of frequencies where one of which, namely, microstrip ring resonator (MRR) method is utilized in this work to extract the dielectric constant and loss tangent of Alumina Ribbon Ceramic in 30-170 GHz. The frequency response of a MRR (S_{21}) has periodic resonant peaks where ε_r is extracted from the locations of resonant peaks while the extraction of the $\tan\delta$ is a function of the quality factor of the peaks. MRRs with the impedance of 68 Ω are designed using following equation [4]:

$$f_0 = \frac{nc}{2\pi r_m \sqrt{\varepsilon_{eff}}} \tag{1}$$

where f_0, r_m, ε_{eff}, and c are the nth resonant frequency of the ring, mean radius of the ring, effective dielectric constant of the substrate, and speed of light in vacuum, respectively. To extract the electrical properties of Alumina Ribbon Ceramic at more resonant frequencies, three MRRs operating at the fundamental frequencies of 10, 15, and 20 GHz are designed. MRRs are fed by microstrip feedlines of 68 Ω impedance and probed using CBCPW-to-MS transitions put at both ends of MRRs. These via-less transitions are designed based on the design rules in [14], compatible with the probe pitches used for measurements in 30-110 GHz and 110-170 GHz which are 200 µm and 75 µm, respectively. To extract the response of MRR, the Thru-Reflect-Line (TRL) structures are also designed to remove the effects of probe pads, CBCPW-to-MS transitions, and feedlines. Fig. 1 shows the material stack-up used for MRR designs along with the layout of MRRs, given designed dimensions listed in Table I. The targeted copper thickness in the design process of all structures is chosen to be 6 µm.

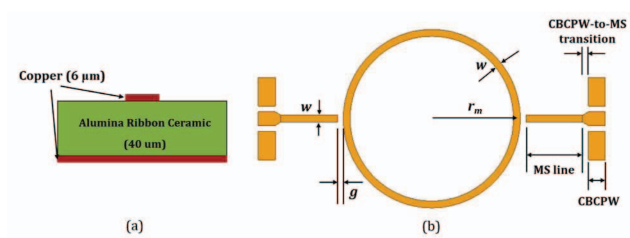

Fig. 1. (a) Material stack-up for MRR designs. (b) layout of MRR designs.

TABLE I. DESIGN PARAMETERS OF MRRS

Design Parameters	Value		
	10-GHz MRR	*15-GHz MRR*	*20-GHz MRR*
r_m	1900 µm	1268 µm	952 µm
g	10 µm	10 µm	10 µm
w	13 µm	13 µm	13 µm

B. Microstrip and CPW Transmission Lines

Transmission lines are designed in Keysight Advanced Design System (ADS) considering the probe pitches, desired impedances, and ease of fabrication for the line width and gap. Microstrip lines with 68 Ω impedance designed on the material stack-up shown in Fig. 1(a) yields the line width of 13 µm, as presented in Table I. In the design process of MRRs and microstrip lines, higher impedance than 50 Ω is targeted to mitigate the effect of frequency dispersion at higher frequencies [7]. Considering the process variations during the fabrication process, the microstrip line width is set to 13 µm to ensure the fabrication tolerances within an acceptable range. As with MRRs, CBCPW-to-MS transitions are put at both ends of microstrip lines to measure them in 30-170 GHz. The MS line insertion loss is extracted after de-embedding the measured results using TRL structures.

CPW lines are designed corresponding to the probe pitches used for measurements below 110 GHz and in 110-170 GHz. The material stack-up and the layout for CPW line designs are shown in Fig. 2, along with the design parameters given in Table II, from which the impedances of CPW lines are calculated to be 60 Ω and 52.8 Ω for the respective frequency bands.

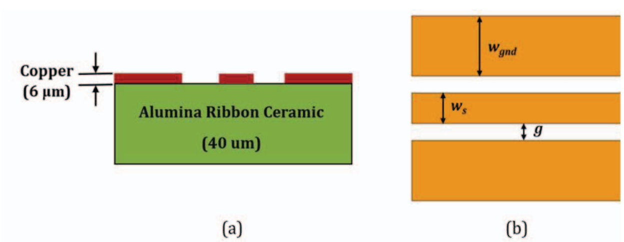

Fig. 2. (a) Material stack-up for CPW line designs. (b) layout of CPW line designs.

TABLE II. DESIGN PARAMETERS OF CPW LINES

Design Parameters	Value	
	30-110 GHz	*110-170 GHz*
w_s	90 µm	45 µm
w_{gnd}	250 µm	100 µm
g	50 µm	27 µm

III. FABRICATION PROCESS

The designed structures are fabricated using the SAP process [15]. The fabrication process starts with a bare 40-µm-thick Alumina Ribbon Ceramic panel where a seed layer of Titanium/Copper (50nm/150nm) is deposited on both sides of the panel using physical vapor deposition (PVD). Then, a 30-µm-thick dry-film photoresist (PR) is vacuum-laminated on both sides, followed by patterning the panel using standard photolithography process. After PR development and electroplating the panel to achieve the desired copper thickness, the PR is stripped, and deposited seed layer (Ti/Cu) is etched away to obtain the final circuits of structures. The fabricated panel is inspected using Zeta Optical Profilometer. From the measured dimensions of fabricated structures, the width (w) of MS line and the gap (g) of MRRs show a maximum variation of 1.7 µm and -0.8 µm, respectively. In addition, the variations for the width (w_s) of CPW lines are measured to be 3.1 µm and 2.6 µm for 30-110 GHz and 110-170 GHz, respectively, whereas the gap (g) of CPW lines decreases by 2.8 µm and 2.6 µm for the respective frequency bands. Overall, the measured dimensions demonstrate the high accuracy of fabrication process with tolerances controlled in a strict region. The realized copper thickness is measured to be 7 µm and the measured rms value of surface roughness is 70 nm which is less than the copper skin depth at 170 GHz (160.3 nm). The fabricated structures on Alumina Ribbon Ceramic are depicted in Fig. 3.

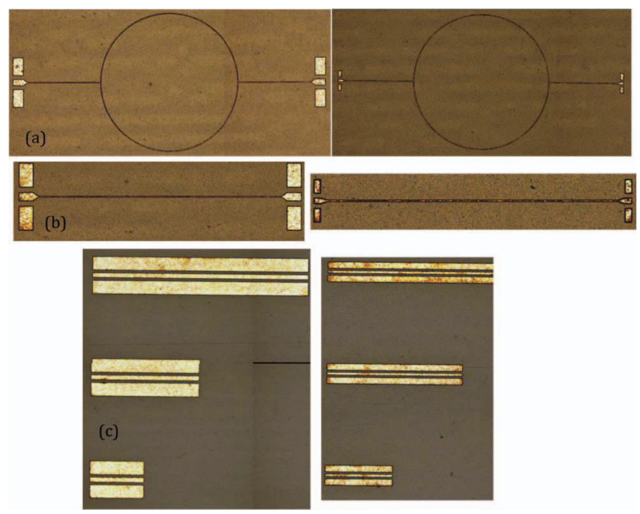

Fig. 3. Fabricated structures on Alumina Ribbon Ceramic substrate: (a) 20-GHz MRRs for 30-110 GHz (left) and D-band (right); (b) MS lines for 30-110 GHz (left) and D-band (right); (c) CPW lines for 30-110 GHz (left) and D-band (right).

IV. MEASUREMENT RESULTS

To characterize the fabricated structures up to 170 GHz, two different measurement setups are utilized corresponding to each frequency band of interest. Anritsu VNA (ME7808) and the frequency extenders 3742A-EW along with the Cascade MicroTech ACP-110-GSG-200 probes are used to cover the frequency range of 30-110 GHz while Agilent E8361C VNA together with millimeter wave controller and frequency extenders (V06VNA2) are used to measure the structures with infinity probes 170-S-GSG-75-BT in 110-170 GHz. All measurements are carried out under Line-Reflect-Reflect-Match (LRRM) calibration using WinCal software. Good calibration is ensured for both measurement setups as the thru standard varies up to ± 0.1 dB in the whole range of frequency bands. The measured scattering parameters of MRRs and transmission lines are presented and analyzed in the following subsections.

A. Microstrip Ring Resonators

Multiple coupons were fabricated and measured for each of three designed MRRs to compensate for any process variations and statistical errors induced during fabrication and measurement steps. As an example, Fig. 4 shows the measured insertion loss (S_{21}) of three coupons (C1, C2, and C3) for each MRR after applying TRL calibration in 75-110 GHz. As seen, the measured results of coupons are repeatable and exhibit good correlation, proving the robustness of fabrication process. Electrical properties of Alumina Ribbon Ceramic are extracted from measured MRRs in 30-170 GHz.

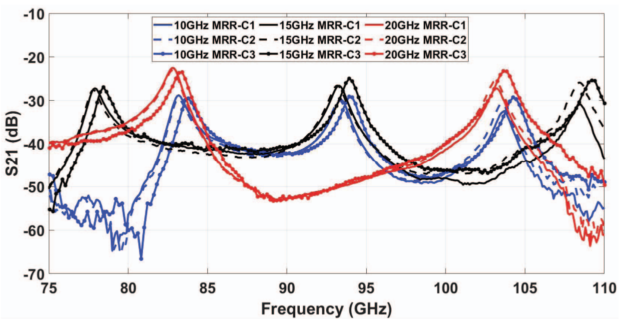

Fig. 4. S_{21} measurements of fabricated MRRs for different coupons after TRL calibration.

1) Dielectric constant of Alumina Ribbon Ceramic: at each resonant frequency of a given MRR, the effective permittivity (ε_{eff}) can be calculated using (1). Then, the relative permittivity (ε_r) is extracted using the frequency dispersive model of effective permittivity due to its accuracy at mm-wave frequencies considering dispersion effects of microstrip lines [4, 16]. The dielectric constant of Alumina Ribbon Ceramic in 30-170 GHz after grouping data points is depicted in Fig. 5, where a confidence interval of 95% is used to represent the uncertainty at each data point as a vertical error bar. From the measured MRRs, $\varepsilon_r = 9.87 \pm 0.031$ is obtained, showing a stable trend around 9.87 in the whole frequency band.

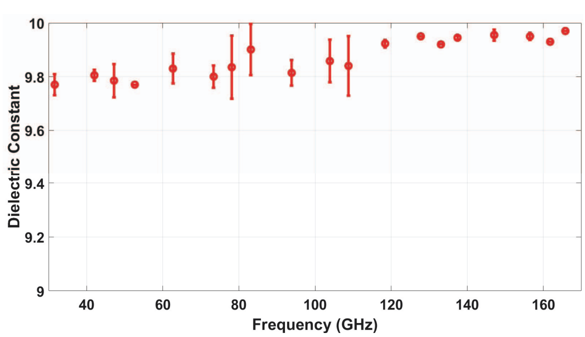

Fig. 5. Extracted dielectric constant of Alumina Ribbon Ceramic from measured MRRs using frequency dispersive model.

The extracted dielectric constant results from all MRRs vary by less than 2.5% in this frequency band considering the minimum and maximum values of ε_r as 9.73 and 9.98, respectively.

2) Loss tangent of Alumina Ribbon Ceramic: the MRR method provides the total loss (α_{total}) at each resonant peak which is comprised of conductor loss (α_c), dielectric loss (α_d), and radiation loss (α_r). For any resonance of a given MRR, the total loss is calculated from its loaded (Q_L) and unloaded quality (Q_u) factors, determined using following equations [17]:

$$Q_L = f_{nth}/BW_{3dB} \tag{2}$$

$$Q_u = Q_L/\left(1 - 10^{S_{21,dB}(f_{nt}\ )/20}\right) \tag{3}$$

where BW_{3d} is the 3-dB bandwidth of the S_{21} resonance peak and $S_{21,dB}$ (f_{nth}) is the measured value of S_{21} in dB at f_{nth}. Afterwards, α_{total} can be calculated using equation (4):

$$\alpha_{total} = \pi/Q_u\lambda_g \tag{4}$$

where λ_g is calculated by following equation:

$$\lambda_g = c/\sqrt{\varepsilon_{eff}(f_{nth})}\, f_{nth} \tag{5}$$

The radiation loss term has been neglected in estimation of Alumina Ribbon Ceramic's loss tangent for two reasons. First one is that all MRRs were designed considering the requirement of $w/r_m \ll 0.2$ which ensures that no radiation loss is produced by MRRs. The second one is that open-ended micristrip feedlines at both ends of MRRs as the main source of radiation loss are removed after TRL calibration [4]. The conductor loss term is calculated theoretically and subtracted from the total loss which gives the dielectric loss in nepers per meter using equation (6):

$$\alpha_d = \alpha_{total} - \alpha_c \tag{6}$$

The conductor loss formula for microstrip lines given in [18] is used in this work where the surface roughness effect is included through applying a correction factor in the conductor strip resistivity. The rms value of 70 nm for the surface roughness is used in the conductor loss calculations. The loss tangent is calculated using equation (7) by applying dielectric loss values from (6) and extracted ε_{eff} and ε_r from the dispersive model.

$$\tan\delta = \frac{\alpha_d\lambda_0\sqrt{\varepsilon_{eff}}(\varepsilon_r - 1)}{\pi\varepsilon_r(\varepsilon_{eff} - 1)} \tag{7}$$

where λ_0 is the free-space wavelength. The extracted loss tangent of Alumina Ribbon Ceramic in 30-170 GHz is plotted in Fig. 6 where the vertical error bars represent the uncertainty of data points with 95% confidence interval. The loss tangent varies from 0.0003 to 0.0013 over 30-170 GHz, exhibiting ultralow loss values in a broad frequency range. This is an important attribute for a packaging material to make efficient modules in sub-THz frequency bands.

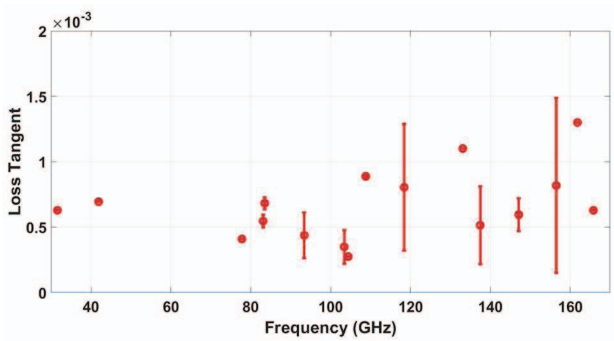

Fig. 6. Extracted loss tangent of Alumina Ribbon Ceramic from measured MRRs.

B. Microstrip and CPW Transmission Lines

Microstrip lines along with TRL structures are measured under LRRM calibration in the frequency bands of 30-110 GHz and 110-170 GHz. To remove the effects of probe pads, CBCPW-to-MS transition, and feedlines and to extract the loss of microstrip line, TRL calibration is applied. Fig. 7 shows the measured scattering parameters of thru and microstrip lines after TRL calibration, where microstrip lines are 3.5 mm and 2.5 mm long against the thru structure in the respective frequency bands. As seen, both thru and microstrip lines are well-matched after TRL across the whole frequency range. The measured insertion loss of microstrip lines changes from 0.089 dB/mm to 0.29 dB/mm in 30-170 frequency band.

To validate the extracted electrical properties of Alumina Ribbon Ceramic in 30-170 GHz, the measured S_{21} of microstrip lines is compared against the simulated results from ANSYS HFSS using the measured dimensions of the lines and extracted ε_r and $\tan\delta$. As shown in Fig. 8, good correlation is obtained for the loss of MS lines in dB/mm over 30-110 GHz and 110-170 GHz, verifying the accuracy of extracted electrical properties of Alumina Ribbon Ceramic.

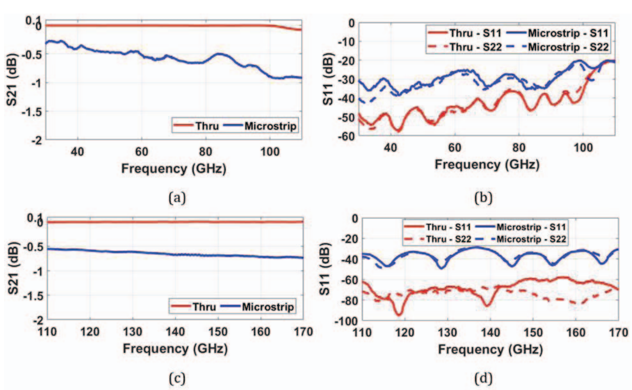

Fig. 7. Measured scattering parameters of thru and microstrip lines after TRL calibration in 30-110 GHz (a and b) and in 110-170 GHz (c and d).

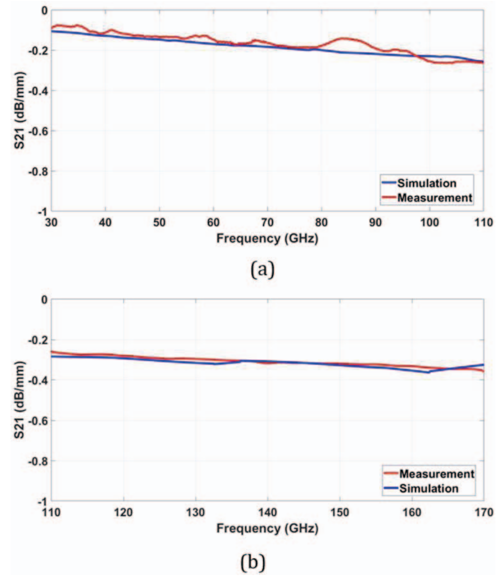

Fig. 8. Correlation of measured and simulated S_{21} (dB/mm) of microstrip lines using extracted electrical properties of Alumina Ribbon Ceramic in 30-110 GHz (a) and 110-170 GHz (b).

CPW lines are also measured under LRRM calibration in 30-170 GHz. As there is not a ground plane on the backside of CPW line and at the measurement setups, they are put in contact with a metal chuck to perform measurements, the CPW line samples are taped on a 1-mm-thick FR4 sheet to ensure isolation from the metal chuck and to provide a solid surface to probe lines successfully as well. Due to high dielectric constant of Alumina Ribbon Ceramic, FR4 sheet should not affect the loss of CPW lines very much. Fig. 9 present the measured scattering parameters of two coupons of CPW lines in 30-110 GHz and 110-170 GHz, respectively, where CPW lines of 8-mm and 10-mm lengths were measured in the respective frequency bands. As seen, the results of different coupons show consistency and minimal differences throughout both frequency ranges. In addition, all lines exhibit good matching in the whole frequency ranges. Based on these measurements, the average insertion loss per unit length (dB/mm) for CPW lines in 30-170 GHz varies from 0.053 dB/mm to 0.242 dB/mm.

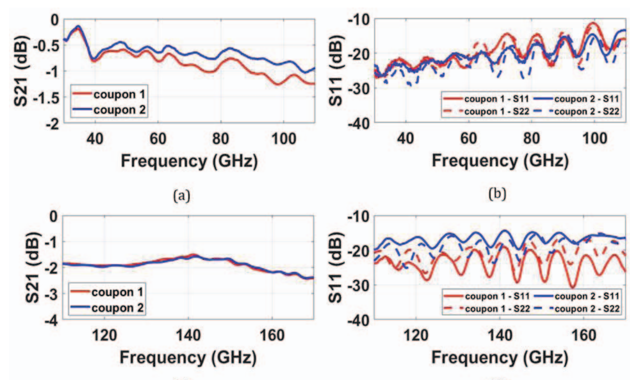

Fig. 9. Measured scattering parameters of CPW lines in 30-110 GHz (a and b) and in 110-170 GHz (c and d) for 8-mm-long and 10-mm-long lines, respectively.

V. COMPARISON OF ALUMINA RIBBON CERAMIC WITH STATE-OF-THE-ART SUBSTRATE TECHNOLOGIES

To evaluate the performance of Alumina Ribbon Ceramic-based interconnects as compared to similar planar transmission lines on the state-of-the-art substrate technologies such as Astra [19], Teflon [19], Rogers [20], LCP [10, 11], and polymer (ABF GL102)/glass (AGC ENA1)/polymer (ABF GL102) [6], a survey is conducted in the literature to extract the insertion loss (dB/mm) of those lines in the frequency range of 30-170 GHz. The comparison results are plotted in Fig. 10. It is worth noting that the geometries of transmission lines compared in Fig. 10 are not identical, considering different substrate technologies. The results indicate that CPW lines on Alumina Ribbon Ceramic represent the superior performance compared to similar lines on other substrates. Moreover, the microstrip lines on Alumina Ribbon Ceramic demonstrate comparable performance with respect to other lines in 30-170 GHz. Table III lists the electrical properties of the substrates in question. As seen, Alumina Ribbon Ceramic substrate represents a very low loss tangent and higher dielectric constant up to 170 GHz compared with other substrates, making it an ideal choice for realizing ultra-miniaturized and highly efficient passive components and packages. In summary, the obtained results denote a unique advantage offered by Alumina Ribbon Ceramic substrates to develop high-performance packages on an ultra-thin material for several applications in 5G and sub-THz bands.

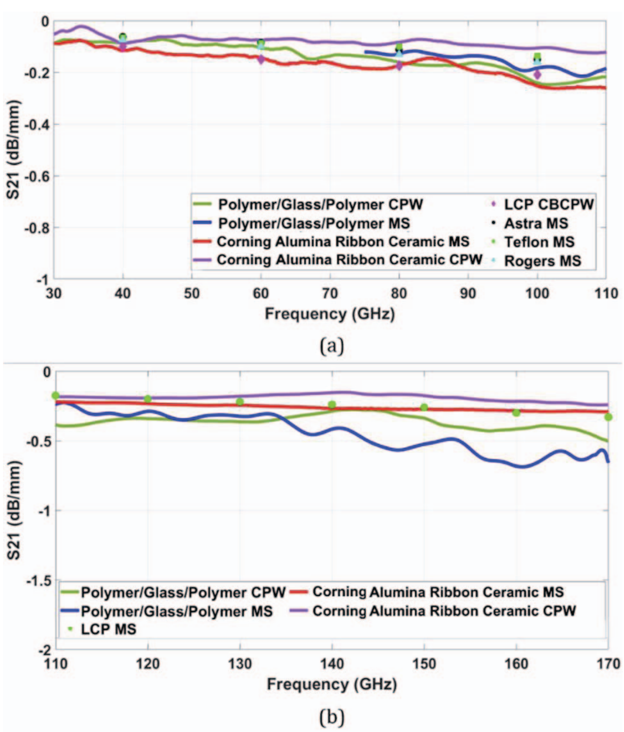

Fig. 10. Comparison of insertion loss (dB/mm) of Alumina Ribbon Ceramic-based interconnects with similar lines on other substrates in 30-110 GHz (a) and 110-170 GHz (b).

TABLE III. COMPARISON OF MATERIAL PROPERTIES OF ALUMINA RIBBON CERAMIC WITH STATE-OF-THE-ART SUBSTRATE TECHNOLOGIES

Substrate Material	ε_r	**tan** δ	f **(GHz)**
Polymer/Glass/Polymer [6]	4.6	0.009 at 103 GHz	75 - 110
LCP [7]	3.16 ± 0.05	0.0045 at 97 GHz	31.53 - 104.6
LCP [8]	3.17	0.0055-0.009	110 - 170
Astra [19]	2.82	0.001	125
Teflon [21]	2.1	0.00028	3
Rogers [22]	2.94	0.0012 at 10 GHz	8 - 40
Alumina Ribbon Ceramic (this work)	9.87 ± 0.03	0.0006 at 165.8 GHz	30 - 170

VI. CONCLUSION

In this paper, electrical properties of the newly developed Alumina Ribbon Ceramic substrate were characterized for the first time in the frequency band of 30-170 GHz using microstrip ring resonator (MRR) method to explore its suitability for potential applications in 5G and 6G frequency bands. From the measured MRRs fabricated using the SAP process, the dielectric constant of a 40-µm-thick Alumina Ribbon Ceramic was extracted to be steady around 9.87 and the loss tangent reaches up to 0.0013 at 161.8 GHz over 30-170 GHz frequency range. Given its excellent electrical properties, Alumina Ribbon Ceramic can be utilized as a core substrate to develop highly efficient and miniaturized passive components and packages required in mm-wave frequency region. Microstrip and CPW transmission lines were designed and fabricated using the SAP process and characterized in 30-170 GHz. Based on the measurements, the average insertion loss of microstrip line varied from 0.089 dB/mm to 0.29 dB/mm in 30-170 GHz. For the CPW lines, the average insertion loss is between 0.053 dB/mm to 0.242 dB/mm in the same frequency range. Furthermore, the comparisons made with other substrate technologies reveal that CPW lines on Alumina Ribbon Ceramic exhibit the lowest insertion loss against similar transmission lines reported in the literature over the frequency range of 30-170 GHz. These results corroborate the effectiveness of Alumina Ribbon Ceramic substrate as a new promising ultra-thin material for 5G and 6G (sub-THz) applications where low loss is an important attribute to have for such applications.

ACKNOWLEDGMENT

This work was supported by Corning Incorporated and the industry consortium at Georgia Tech's 3D Systems Packaging Research Center (PRC). We acknowledge the contribution of Colin Daly, Scott Pollard, Scott Silence, Karan Mehrotra and Gordon Brown for Corning Incorporated for supporting and establishing this research activity.

REFERENCES

[1] A. O. Watanabe, M. Ali, Sk. Y. B. Sayeed, R. R. Tummala, and M. R. Pulugurtha, "A review of 5g front-end systems package integration," *IEEE Transactions on Components, Packaging, and Manufacturing Technology*, vol. 11, no. 1, pp. 118–133, Jan. 2021.

[2] H. Hao, D. Hui, and D. Lau, "Material advancement in technological development for the 5g wirelss communications," *Nanotechnology Reviews*, vol. 9, pp. 683-699, 2020.

[3] M. Giordani, M. Polese, M. Mezzavilla, S. Rangan, and M. Zorzi, "Toward 6g networks: use cases and technologies," *IEEE Communications Magazine*, vol.58, issue. 3, pp. 55-61, Mar. 2020.

[4] W. T. Khan, "Design and development of organically packaged components and modules for microwave and millimeter-wave applications," PhD disseration, Georgia Institute of Technology, USA, Dec. 2014.

[5] W. T. khan, J. Tong, S. Sitaraman, V. Sundaram, R. Tummala, and J. Papapolymerou, "Characterization of electrical properties of glass and transmission lines on thin glass up to 50 GHz", *IEEE 65th Electronics Components and Technology Conference (ECTC)*, pp. 2138-2143, May 2015.

[6] M. U. Rehman, S. Ravichandran, S. Erdogan, and M. Swaminathan, "W-band and D-band transmission lines on glass- based substrates for sub-THz modules", *IEEE 70th Electronics Components and Technology Conference (ECTC)*, pp. 660-665, May 2020.

[7] D. C. Thompson, O. Tantot, H. Jallageas, G. E. Ponchak, M. M. Tentzeris, and J. Papapolymerou, "Characterization of liquid crystal polymer (LCP) material and transmission lines on LCP substrates from 30 to 110 GHz", *IEEE Transaction on Microwave Theory and Techniques*, vol. 52, no. 4, pp. 1343-1352, Apr. 2004.

[8] W. T. Khan, C. A. D. Morcillo, A. C. Ulusoy, and J. Papapolymerou, "Characterization of Liquid Crystal Polymer from 110 GHz to 170 GHz", *IEEE Radio and Wireless Symposium (RWS)*, pp. 157-159, Jan. 2014.

[9] S. Adhikari, A. Stelzer, A. Springer, C. Wagner, C. Korden and M. Stadler, "Characterization of LTCC substrate up to 100 GHz", *International Conference on Microwave and Millimeter Wave Technology*, pp. 1-4, Apr. 2008.

[10] D. Thompson, P. Kirby, J. Papapolymerou, and M. M. Tentzeris, "W-band characterization of finite ground coplanar transmission lines on liquid crystal polymer (LCP) substrates," *IEEE 53rd Electronics Components and Technology Conference (ECTC)*, pp. 1652-1655, May 2003.

[11] W. T. Khan, A. C. Ulusoy, and J. Papapolymerou, "D-band characterization of co-planar wave guide and microstrip transmission lines on Liquid Crystal Polymer", *IEEE 63rd Electronics Components and Technology Conference (ECTC)*, pp. 2304-2309, May 2013.

[12] C. Zhuang, Y. Wang, L. Cai, J. Markley, H. Vanselous, N. Zhelev, S. -H. Seok, L. Kester, and M. Badding, "Flexibility matters: high purity, thin, flexible alumina ribbon ceramic," *Ceramic & Glass Manufacturing*, vol. 1, no. 4, Sep. 2020.

[13] ANSYS. ANSYS HFSS Ver. 2019.3. Accessed: Jul. 15, 2020. [Online]. Available: http://www.ansys.com

[14] G. Zheng, J. Papapolymerou, and M. M. Tentzeris, "Wideband coplanar waveguide rf probe pad to microstrip transitions without via holes," *IEEE Microwave and Wirelss Components Letters*, vol. 13, no. 12, pp. 544-546, Dec. 2003.

[15] H. Akahoshi, M. Kawamoto, T. Itabashi, O. Miura, A. Takahashi, S. Kobayashi, M. Miyazaki, T. Mutoh, M. Wajima, and T. Ishimaru, "Fine line circuit manufacturing technology with electroless copper plating," *IEEE Transactions on Components, Packaging, and Manufacturing Technology – Part A*, vol. 18, no. 1, pp. 127–135, Mar. 1995.

[16] M. Kirschning, and R. H. Jansen, "Accurate model for effective dielectric constant of microstrip with validity up to millimeter-wave frequencies," Electronics Letters, vol. 18, no. 5, pp. 272-273, Mar. 1982.

[17] C. A. D. Morcillo, "Development of lightweight and low-cost microwave components for remote-sensing applications," PhD disseration, Georgia Institute of Technology, USA, May 2013.

[18] R. Garg, I. Bahl, and M. Bozzi, *Microstrip Lines and Slotlines*, 3rd ed. Boston, MA: Artech House, 2013, pp. 1-589.

[19] Astra MT77, A Teflon Replacement, Isola, July 2017.

[20] F. Fesharaki, T. Djerafi, M. Chaker, and K. Wu, "Guided-wave properties of mode-selective transmission line," *IEEE Access*, vol. 6, pp. 5379-5392, Feb. 2018.

[21] Dielectric Constant, Strength, & Loss Tangent, Accessed: Aug. 4, 2020. [online]. Available: https://www.rfcafe.com/references/electrical/dielectric-constants-strengths.htm.

[22] Rogers Corporation, RT/duroid 6002 high frequency laminates datasheet, [online]. Available: https://rogerscorp.com